Basic Res Cardiol (2016) 111:4
DOI 10.1007/s00395-015-0523-4

ORIGINAL CONTRIBUTION

Persistent increases in Ca^{2+} influx through Cav1.2 shortens action potential and causes Ca^{2+} overload-induced afterdepolarizations and arrhythmias

Xiaoying Zhang[1,2] · Xiaojie Ai[2,6] · Hiroyuki Nakayama[3] · Biyi Chen[4] · David M. Harris[5] · Mingxin Tang[2] · Yuping Xie[4] · Christopher Szeto[2] · Yingxin Li[2] · Ying Li[2,7] · Hongyu Zhang[2] · Andrea D. Eckhart[8] · Walter J. Koch[9] · Jeffery D. Molkentin[3] · Xiongwen Chen[1,2]

Received: 9 October 2015 / Accepted: 19 November 2015 / Published online: 26 November 2015

Abstract Persistent elevation of Ca^{2+} influx due to prolongation of the action potential (AP), chronic activation of the β-adrenergic system and molecular remodeling occurs in stressed and diseased hearts. Increases in Ca^{2+} influx are usually linked to prolonged myocyte action potentials and arrhythmias. However, the contribution of chronic enhancement of Cav1.2 activity on cardiac electrical remodeling and arrhythmogenicity has not been completely defined and is the subject of this study. Chronically increased Cav1.2 activity was produced with a cardiac specific, inducible double transgenic (DTG) mouse system overexpressing the β2a subunit of Cav (Cavβ2a). DTG myocytes had increased L-type Ca^{2+} current ($I_{Ca\text{-}L}$), myocyte shortening, and Ca^{2+} transients. DTG mice had enhanced cardiac performance, but died suddenly and prematurely. Telemetric electrocardiograms revealed shortened QT intervals in DTG mice. The action potential duration (APD) was shortened in DTG myocytes due to significant increases of potassium currents and channel abundance. However, shortened AP in DTG myocytes did not fully limit excess Ca^{2+} influx and increased the peak and tail $I_{Ca\text{-}L}$. Enhanced I_{Ca} promoted sarcoplasmic reticulum (SR) Ca^{2+} overload, diastolic Ca^{2+} sparks and waves, and increased NCX activity, causing increased occurrence of early and delayed afterdepolarizations (EADs and DADs) that may contribute to premature ventricular beats and ventricular tachycardia. AV blocks that could be related to fibrosis of the AV node were also observed. Our study suggests that increasing $I_{Ca\text{-}L}$ does not necessarily result in AP prolongation but causes SR Ca^{2+} overload and fibrosis of AV node and myocardium to induce cellular arrhythmogenicity, arrhythmias, and conduction abnormalities.

Keywords L-type calcium channel or Cav1.2 · β_{2a} subunit · Afterdepolarizations · Short QT · Potassium currents

X. Zhang and X. Ai contributed equally to this study.

Electronic supplementary material The online version of this article (doi:10.1007/s00395-015-0523-4) contains supplementary material, which is available to authorized users.

✉ Xiongwen Chen
xchen001@temple.edu

[1] Daping Hospital, The Third Military Medical University, Chongqing, China

[2] Cardiovascular Research Center and Department of Physiology, Temple University School of Medicine, Philadelphia, PA 19140, USA

[3] Cincinnati Children's Hospital Medical Center, Department of Pediatrics, University of Cincinnati, Cincinnati, OH 45229, USA

[4] Department of Internal Medicine, University of Iowa, Iowa City, IA 52242, USA

[5] College of Medicine, University of Central Florida, Orlando, FL 32827, USA

[6] School of Agriculture and Biology, Shanghai Jiao Tong University, Shanghai 200240, China

[7] The Second Artillery General Hospital, Beijing 100088, China

[8] MedThink SciCom, Raleigh, NC 27609, USA

[9] Center for Translational Medicine and Department of Pharmacology, Temple University School of Medicine, Philadelphia, PA, USA

Abbreviations

4-AP	4-Aminopyridine
AP	Action potential
APD	Action potential duration
CaMK II	Ca^{2+}/Calmodulin-dependent kinase II
Cavβ2a	The β2a splicing variant of the β2 subunit of the L-type Ca^{2+} channel
DAD	Delayed afterdepolarization
DTG	Double transgenic
EAD	Early afterdepolarization
ECG	Electrocardiography
ECHO	Echocardiography
FDHM	Full duration at half maximum
FWHM	Full width at half maximum
$I_{Ca\text{-}L}$	L-type Ca^{2+} current
LTCC or Cav1.2	The L-type Ca^{2+} channel
NCX	Na^{+}/Ca^{2+} Exchange
NFAT	Nuclear factor of activated T-cells
PKA	Protein kinase A
QTc	Corrected QT interval
SQTS	Short QT syndrome
RyR2	Ryanodine receptor type 2
SR	Sarcoplasmic reticulum

Introduction

Cardiac arrhythmias are a significant contributor to premature death in the United States. Aberrant Ca^{2+} homeostasis and electrical remodeling are central to cardiac arrhythmias [1, 2]. Altered properties of the L-type Ca^{2+} channel (LTCC or Cav1.2) play important roles in cardiac arrhythmias because it is linked to both the electrical properties and Ca^{2+} homeostasis [2]. The L-type Ca^{2+} current ($I_{Ca\text{-}L}$) determines the duration of the action potential and provides the source of Ca^{2+} for loading the sarcoplasmic (SR) [2, 6]. β-Adrenergic stimulation [2, 12] or gene mutations [20] or changes of the subunit composition [21] of the L-type Ca^{2+} channel may increase the activities of the LTCC. The dogma is that increases in $I_{Ca\text{-}L}$ cause the prolongation of the action potential duration (APD) and SR Ca^{2+} overload in patients [2] and animals [15]. While action potential prolongation provides a substrate for early afterdepolarizations (EADs), spontaneous Ca^{2+} release from the SR with Ca^{2+} overload induces delayed afterdepolarizations (DADs). Both EADs and DADs are triggers for cardiac arrhythmias [17]. AP prolongation and increased Cav1.2 activity may lead to reopening of Cav1.2 during the plateau of APs to induce EADs. Mutations of Cav1.2 that increase Cav1.2 activity induce a long QT syndrome in human [20]. Increases in Ca^{2+} influx elevate cytosolic and SR Ca^{2+}, which could decrease the expression of the transient outward potassium channels [28]. However, the resultant remodeling of electrical properties and Ca^{2+} handling of myocytes when Cav1.2 activity is chronically increased has not been fully characterized and is the topic of this study.

To simulate increases in Cav1.2 activity, we overexpressed the β2a subunit of Cav (Cavβ2a) in a cardiac specific and inducible manner in mice [11, 25]. In this transgenic (TG) mouse system, overexpression of $Cav\beta_{2a}$ elicited the same modulatory effect on Cav1.2 activity (mode 2) as does phosphorylation of Cav1.2. Along with increased Ca^{2+} influx into cardiomyocytes and enhanced cardiac contractility in Cavβ2a TG mice, the QT intervals and ventricular myocyte APDs were decreased, in contrast to prolonged QT and APD typically observed with increased Cav1.2 activity [20]. This is because of compensatory increases in potassium currents due to increased expression of multiple potassium channels. On top of shortened APs, EADs and DADs were still detected, which could be associated with increased peak and tail $I_{Ca\text{-}L}$, high SR Ca^{2+} load and leak, and increased NCX activity in Cavβ2a TG myocytes. Telemetric ECG showed AV blocks, premature ventricular contraction, and non-sustained monomorphic ventricular tachycardia in DTG mice which could be related to SR Ca^{2+} overload, cardiac hypertrophy, and fibrosis. Our study suggests that the increases in the L-type Ca^{2+} channel activity do not necessarily prolong the action potential but cause SR Ca^{2+} overload and myocardial fibrosis to induce EADs, DADs, arrhythmias, and conduction abnormalities, at least in mice.

Methods

Detailed method description is included in the supplemental material. A transgenic mouse line overexpressing Cavβ2a at relatively low expression level and Cav1.2α1 knockout mouse were used for this study [11, 19, 25] (Supplemental Fig. 1). Animal studies were approved by the Institutional Animal Care and Use Committee of Temple University.

Left ventricular myocytes (LVMs) were isolated and whole cell L-type Ca^{2+} current ($I_{Ca\text{-}L}$) and sodium–calcium exchange current (I_{NCX}) were measured [25]. Action potentials (APs) and Ca^{2+}-insensitive potassium currents were measured in myocytes from the midwall of the free wall of the left ventricle [13]. Diastolic Ca^{2+}, Ca^{2+} transients and SR Ca^{2+} load were measured with the fluorescent Ca^{2+} indicators indo-1-AM or Fluo-4 AM [25]. Line scan Ca^{2+} transients were also recorded by confocal (LSM510 confocal microscope, Carl Zeiss MicroImaging)

line scanning [33]. ECHO was performed with a VisualSonics Vevo 770 machine [35]. Implanted ETA-F20 telemetric transmitters (DSI, St. Paul, MN) were used to record ECG in 6-month-old mice. Masson's trichrome staining was performed to determine fibrosis of myocardium and AV node [10, 25, 34]. Western blot procedure was performed to detect protein abundance. Twenty control and 20 DTG mice receiving standard care by the Central Animal Facility at Temple University were observed daily during a 12-month period for survival.

Data are reported as mean ± SEM. Paired and unpaired *t* test, Kaplan–Meier's survival test and contingency table analysis for incidence rates were performed with GraphPad Prism 5.0. ANOVA or ANOVA for repeated measures were used to detect significance with SAS 9.0 (SAS Institute Inc., Cary, NC). A p value of ≤ 0.05 was considered significant.

Results

Cavβ2a overexpression increased $I_{Ca\text{-}L}$, Ca^{2+} transient amplitudes, and contractions in VMs

In myocytes isolated from 6-month-old DTG mice, we found that $I_{Ca\text{-}L}$ was significantly increased by 82.0 % versus wild-type mice (maximum $I_{Ca\text{-}L}$: control 12.8 ± 0.8 vs. DTG 23.2 ± 2.2 pA/pF) (Fig. 1a, b). The amplitudes of Ca^{2+} transients and contractions induced by field stimulation at 0.5 Hz were also significantly increased, while the diastolic Ca^{2+} concentration was not altered in the DTG myocytes (Fig. 1c–e). These data agree with our previous study in 4-month-old DTG [25].

Cavβ2a DTG mice had enhanced cardiac function but died prematurely and suddenly

Consistent with increased myocyte function in DTG hearts, DTG hearts had enhanced function (ejection fraction) than WT hearts during the 4–12 months of life (Fig. 2a–c). However, DTG mice began to die suddenly after the age of 4 months, which corresponds to the time when Cavβ2a expression is detectable [25] (Fig. 2d). These data show that DTG mice did not die from depressed cardiac function, and suggest an arrhythmic mechanism for the sudden death.

Cavβ2a DTG mice had shortened QT intervals

Telemetric ECGs showed that the QT interval and heart rate corrected QT interval (QTc) were significantly shorter in DTG with increased $I_{Ca\text{-}L}$ than in control mice (Fig. 2), which is opposite to the anticipated longer QT interval usually seen with gain of function of Cav1.2 in humans [20]. After the control and DTG mice were treated with verapamil for 8 weeks since the age of 4 months, QT and QTc were not different between control and DTG mice although in both groups of animals, QT and QTc were shortened due to the blockade of the L-type channel by verapamil (Fig. 3c, d).

Cavβ2a DTG myocytes had shorter action potentials due to increased potassium currents

QT interval represents the average AP duration of ventricular myocytes. Therefore, APs were measured in isolated VMs to determine the bases of the shortened QT intervals [20]. While there was no significant difference in resting membrane potentials (control vs. DTG: −66.6 ± 1.5 vs. −65.3 ± 2.1 mV, without correction for the junction potential) and the overshoot amplitudes of the action potentials (control vs. DTG: 26.6 ± 3.8 vs. 30.6 ± 3.3 mV, without correction for the junction potential), APD50, APD75, and APD90 were significantly shorter in DTG myocytes than in control myocytes (Fig. 4a, b). The maximal phase 1 decay rate, an index of transient outward potassium current (I_{to}), was significantly increased in DTG myocytes (Fig. 4c). These alterations of action potentials in DTG myocytes were normalized by feeding the DTG mice with verapamil (Fig. 4a–c), suggesting that these changes were induced by increased Ca^{2+} influx rather than a direct effect of the overexpressed Cavβ2a.

The balance between depolarizing $I_{Ca\text{-}L}$ and repolarizing potassium currents determines APD [5], and we observed shortened APDs even though $I_{Ca\text{-}L}$ was increased in DTG VMs. Therefore, we anticipated increased outward K^+ currents (I_K) in DTG myocytes. The peak amplitude of total I_K was significantly greater in DTG VMs than in control VMs (Fig. 4d–f). The 4-AP-insensitive I_{SUS}/I_{K1} [26] density in DTG VMs was greater than in control VMs (Fig. 4g–i). The 4-AP-sensitive potassium currents (mostly I_{to} and $I_{K,slow1}$) [26] density was also greater in DTG VMs than in control VMs at test potentials >0 mV (Fig. 4j–l). The increases in both 4-AP-sensitive and 4-AP-insensitive potassium currents suggest that chronically elevated Ca^{2+} influx induces a compensatory upregulation of multiple potassium channel currents. The increases of total K^+ currents, 4-AP-insensitive K^+ currents and 4-AP-sensitive K^+ currents in DTG myocytes were normalized by treating DTG mice with verapamil (Fig. 4f, i and l), arguing against a direct modulatory effect of overexpressed Cavβ2a on K^+ channel expression.

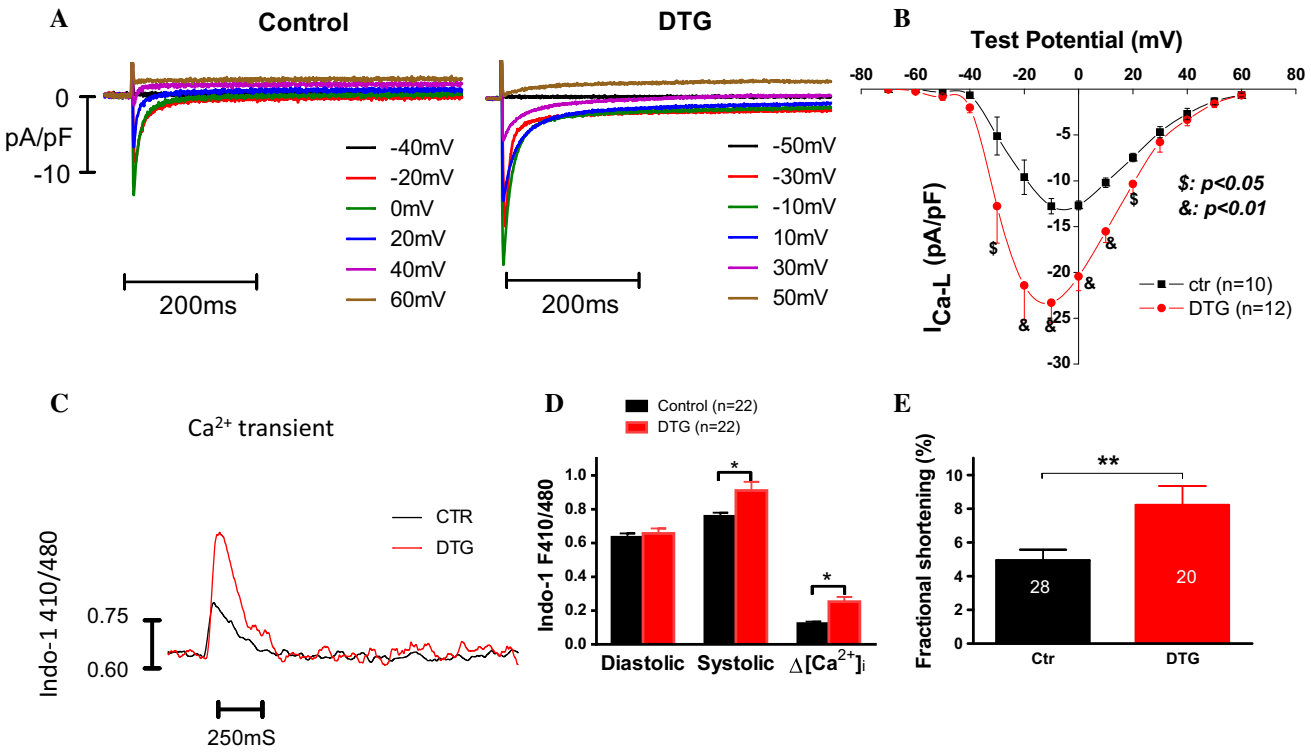

Fig. 1 DTG myocytes have greater $I_{Ca\text{-}L}$ density and enhanced contractility. **a** Raw $I_{Ca\text{-}L}$ recordings in a control VM and a DTG VM. **b** Current–voltage (*I–V*) relationships of $I_{Ca\text{-}L}$ in control (ctr, $n = 10$, $N = 3$) and DTG ($n = 12$, $N = 3$) VMs. **c** Examples of Ca^{2+} transients in a control and a DTG VM. **d** Diastolic, systolic and the amplitude of $[Ca^{2+}]_i$ measured with indo-1 in control and DTG VMs recorded at 0.5 Hz, showing no difference in diastolic but increased systolic amplitudes of $[Ca^{2+}]_i$ in DTG VMs. **e** Greater myocyte contraction expressed as fractional shortening was observed in DTG VMs. $^{\$}p < 0.05$, $^{\&}p < 0.01$, control vs. DTG at the same test potential, two-way ANOVA with post hoc *t* tests; $^{*}p < 0.05$, $^{**}p < 0.01$ control vs. DTG, student *t* test. "*n*" cells from "*N*" animals were studied

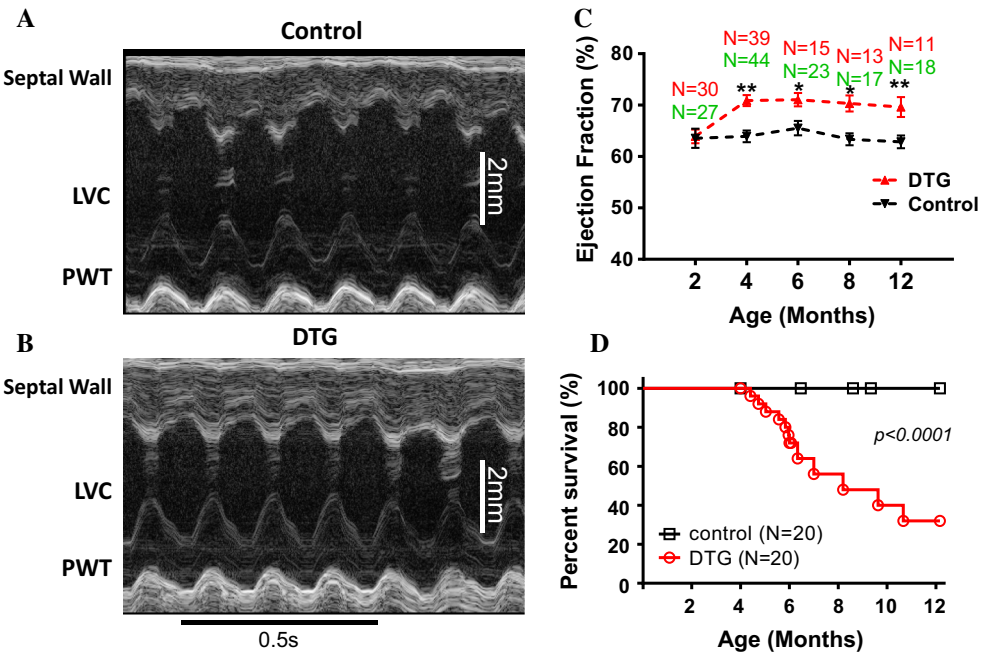

Fig. 2 DTG mice have hypercontractile hearts but die suddenly after transgene expression. Examples of M-mode images of echocardiography of a control mouse (**a**) and a DTG (**b**) mouse at the age of 6 months. **c** Ejection fractions (EF) of control and DTG mice from the age of 2–12 months, showing cardiac hypercontractility in DTG mice at ages ≥4 months. $^{*}p < 0.05$ DTG vs. control; $^{**}p < 0.01$ DTG vs. control; **d** Kaplan–Meier's survival test of control and DTG mice. *N* numbers of animals studied

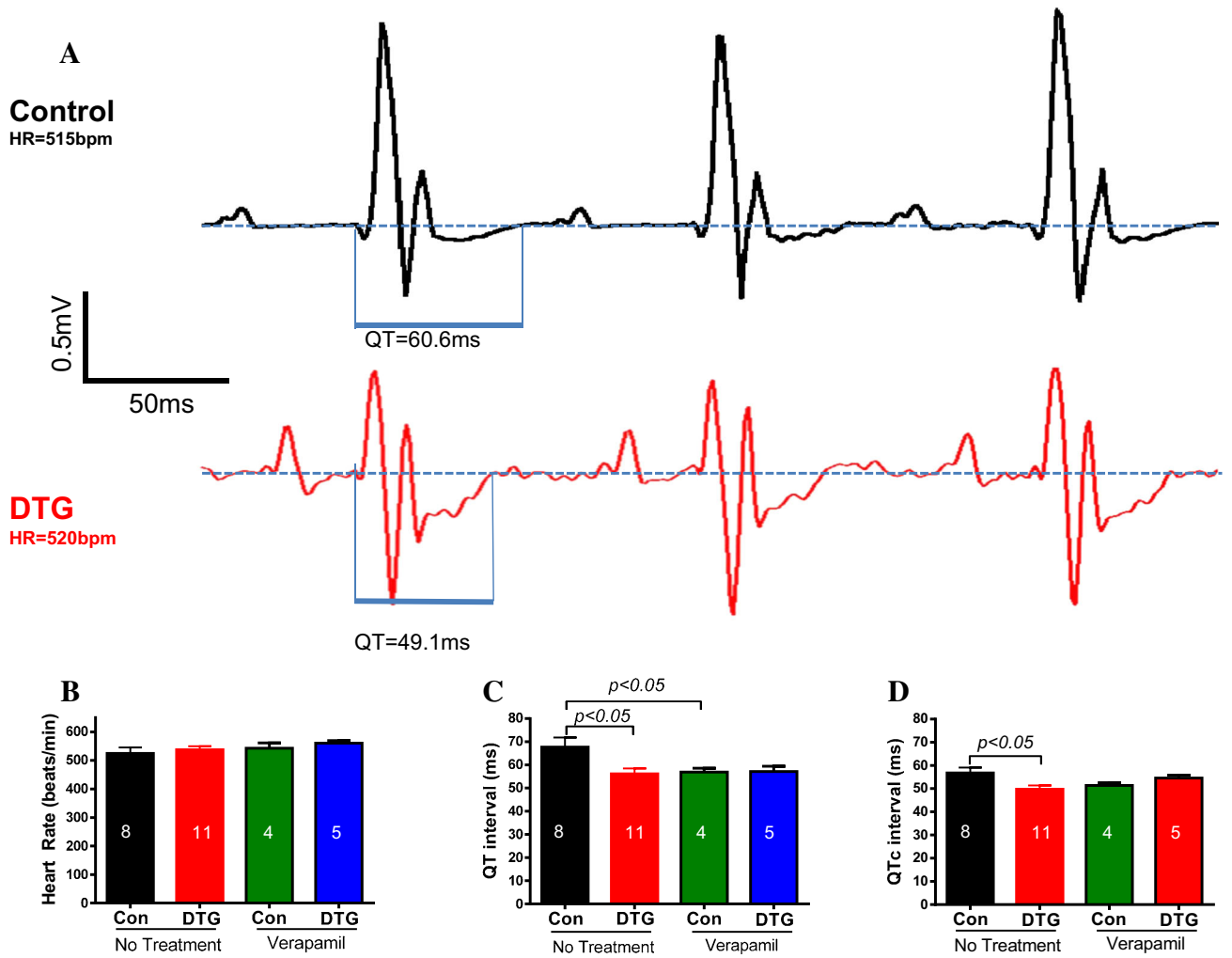

Fig. 3 DTG mice have shortened QT intervals that are normalized by verapamil. **a** Examples of telemetric ECGs recorded from a control and a DTG mice. QT durations are indicated. **b** DTG and control mice with or without verapamil treatment have similar heart rates. QT intervals (**c**) and corrected QT intervals (**d**) are shorter in DTG than in control mice but verapamil treatment shortened QT and QTc to the same in both groups of animals. The *numbers in the bars* are numbers of animals studied

Multiple genes encode the channels that mediate I_{to}: KCNA4 encodes $K_v1.4$ ($I_{to,s}$); KCND2 and KCND3 encode Kv4.2 and Kv4.3 ($I_{to,f}$), respectively; the accessory subunit KCNIP2 encodes KChIP2 [26]. In DTG hearts, the expression of distinct I_{to} channels was differentially regulated by enhanced Ca^{2+} influx. The protein abundance of Kv4.3 and KChIP2 was significantly increased (Fig. 5). Kv1.4 and Kv4.2 protein abundances were not altered. These data suggest that the increased I_{to} was primarily due to elevated abundance of Kv4.3 and KChIP2. The abundance of Kv2.1, which mediates $I_{K,slow}$, was also significantly increased (Fig. 5). I_{K1} is mediated by Kir2.1 and Kir2.2 channels in mouse hearts. In the DTG hearts, the protein abundance of Kir2.1 was not changed but Kir2.2 was significantly increased (Fig. 5), indicating that the increase in Kir2.2 abundance accounts for the larger I_{K1} in DTG myocytes.

Shortened AP did not effectively limit Ca^{2+} influx but increased I_{Ca} peak and tail currents in Cavβ2a DTG myocytes

Our data suggest that APD shortening could be an adaptive mechanism for limiting Ca^{2+} influx into the myocytes to decrease the potential detrimental effects of cellular Ca^{2+} overload in DTG myocytes. To determine if the shortened APD in DTG myocytes effectively reduced $I_{Ca\text{-}L}$ to normal levels, $I_{Ca\text{-}L}$ was measured with the action-potential clamp

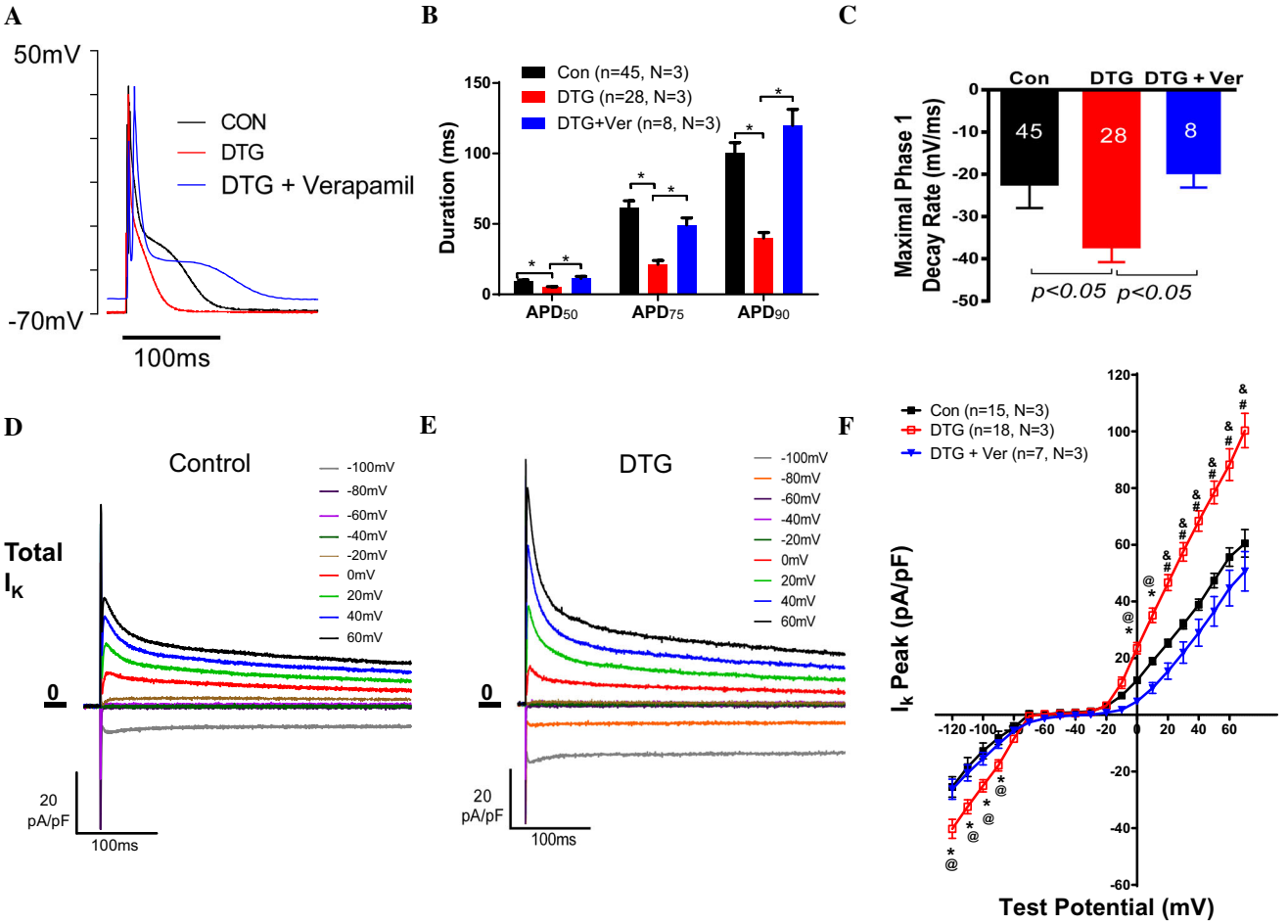

Fig. 4 DTG myocytes have shortened AP duration and increased potassium currents that can be reversed by verapamil treatment. Typical APs (**a**), AP durations (APDs) (**b**), and maximal phase 1 decay rates of APs (**c**) recorded in VMs from control, DTG and DTG with verapamil treatment mice. **d**, **e** Examples of total I_K recorded in control and DTG VMs. **f** Averaged I_K peak in VMs of control, DTG and DTG+ verapamil animals at different testing potentials. **g**, **h** Examples of 4-AP-insenstive K^+ currents from a control and a DTG myocytes. **i** Averaged sustained 4-AP-insensitive K^+ currents in VMs of control, DTG and DTG+ verapamil animals at the end of the 4 s at different test potentials. **j** and **k** Examples of 4-AP-senstive K^+ currents from a control VM and a DTG VM. **l** Averaged 4-AP-sensitive K^+ currents in VMs of control, DTG and DTG+ verapamil animals at different test potentials. In **f**, **I**, and **l**: $^*p < 0.05$ DTG vs. control; $^\$p < 0.01$ DTG vs. control; $^\#p < 0.001$ DTG vs. control; $^@p < 0.05$ DTG vs. DTG+ verapamil; $^\%p < 0.01$ DTG vs. DTG+ verapamil; $^\%p < 0.001$ DTG vs. DTG+ verapamil. Repeated two-way ANOVA with post hoc *t* test (15 control VMs from 3 control mice; 18 DTG VMs from 3 DTG mice, 7 VMs from 3 verapamil-treated DTG mice)

technique using representative AP shapes from control and DTG myocytes. Total Ca^{2+} influx with DTG AP clamp was 17–25 % less than with control VM AP clamp in both control and DTG VMs. However, total Ca^{2+} influx through the Cav1.2 channel was 3.1 times greater in DTG VMs with shortened DTG APs than in control VMs with control APs (Fig. 6a, c). Further examination of the I_{Ca} under AP clamp showed that I_{Ca} peak was greater with the shortened DTG AP than with the control AP in both DTG and control VMs (Fig. 6d). The duration of Ca^{2+} currents was shortened with DTG type APs in both control and DTG VMs (Fig. 6a, e) but the amplitudes of the 2nd peak of I_{Ca} under AP clamp were greater than when a normal AP was applied in both control and DTG VMs (Fig. 6b, f). These data imply that shortened AP increases peak and tail $I_{Ca\text{-}L}$, which could contribute to DTG myocyte Ca^{2+} overload and depolarization of myocytes during the plateau phase (phase 1) to predispose DTG VMs to EADs and DADs.

Enhanced Ca^{2+} influx caused SR Ca^{2+} overload and increased diastolic Ca^{2+} spark frequencies and Ca^{2+} waves

Enhancing Ca^{2+} influx through the Cav1.2 channel can cause SR Ca^{2+} overload, which has been considered as a

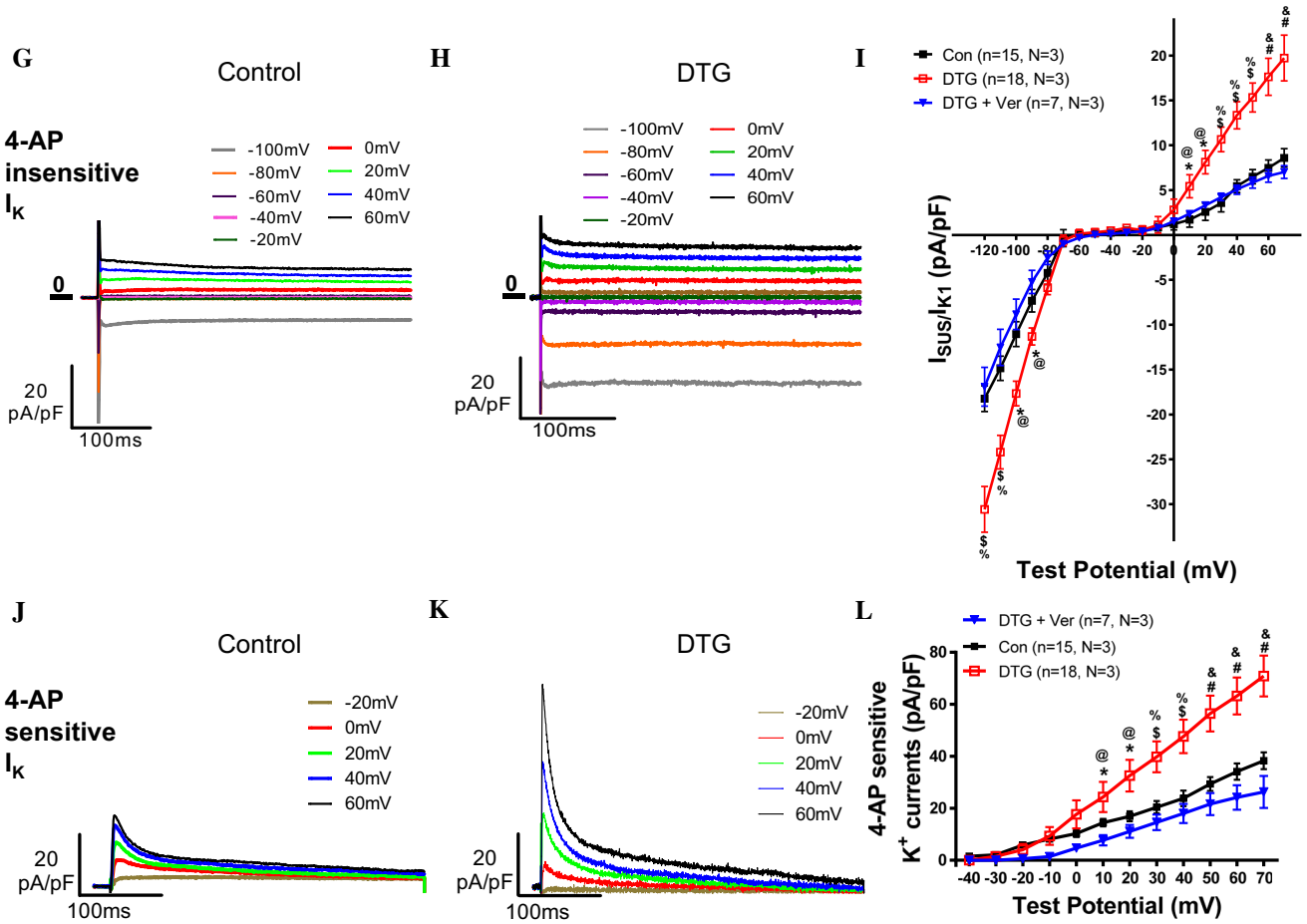

Fig. 4 continued

key event for cellular arrhythmogenicity and causes myocyte death [14, 25]. We found that the SR Ca^{2+} content, indicated by the amplitude of the peak of the caffeine-induced Ca^{2+} transients, was significantly increased in DTG VMs (Fig. 7a, b).

Ca^{2+} overloaded SR tends to spontaneously release its stored Ca^{2+} during diastole which can be measured as spontaneous Ca^{2+} sparks and Ca^{2+} waves. Confocal line scan imaging was used to determine spark frequency within 10 s after stopping field stimulation. No differences were observed in the spark properties: amplitude (F/F_0), full width at half maximum (FWHM), and full duration at half maximum (FDHM) (Supplemental Fig. 2), and Ca^{2+} spark frequency at rest (Fig. 7g) between control and DTG VMs. The Ca^{2+} wave frequency at rest was significantly increased in DTG VMs (Fig. 7h). Under steady state field stimulation, the amplitude of Ca^{2+} transients was greater at both 1 and 3 Hz frequencies in DTG VMs (Fig. 7a; Supplemental Fig. 3). The Ca^{2+} transients of control VMs were quickly decayed and then showed little diastolic Ca^{2+} release, DTG VMs had a high incidence of abnormal diastolic Ca^{2+} release at 3 Hz (Fig. 7c–f, i), which resulted in an elevated diastolic cytosolic Ca^{2+} concentration at this pacing frequency. Diastolic Ca^{2+} release causes depolarization of the membrane potential via the electrogenic Na^+/Ca^{2+} exchanger, resulting in EADs and DADs. I_{NCX} was significantly increased in DTG VMs (Fig. 7j–l).

Cavβ2a DTG myocytes had increased EADs and DADs

Diastolic Ca^{2+} release causes EADs and DADs that underlie arrhythmias [2]. In isolated myocytes, only 3 of the 45 control myocytes had occasional EADs and DADs; in contrast, 8 of 28 DTG VMs had frequent EADs and/or DADs (Fig. 8a–d). Among all APs recorded from the 3 control VMs and the 8 DTG VMs with EADs and/or DADs, we found that the percentage of APs with EADs or DADs was significantly higher in DTG (23.6 ± 4.9 %) than in control VMs (1.5 ± 0.6 %) (Fig. 8e). Furthermore, multiple EADs (Fig. 8b, arrows) and DADs (Fig. 8c, arrows) were often observed together in one AP from DTG

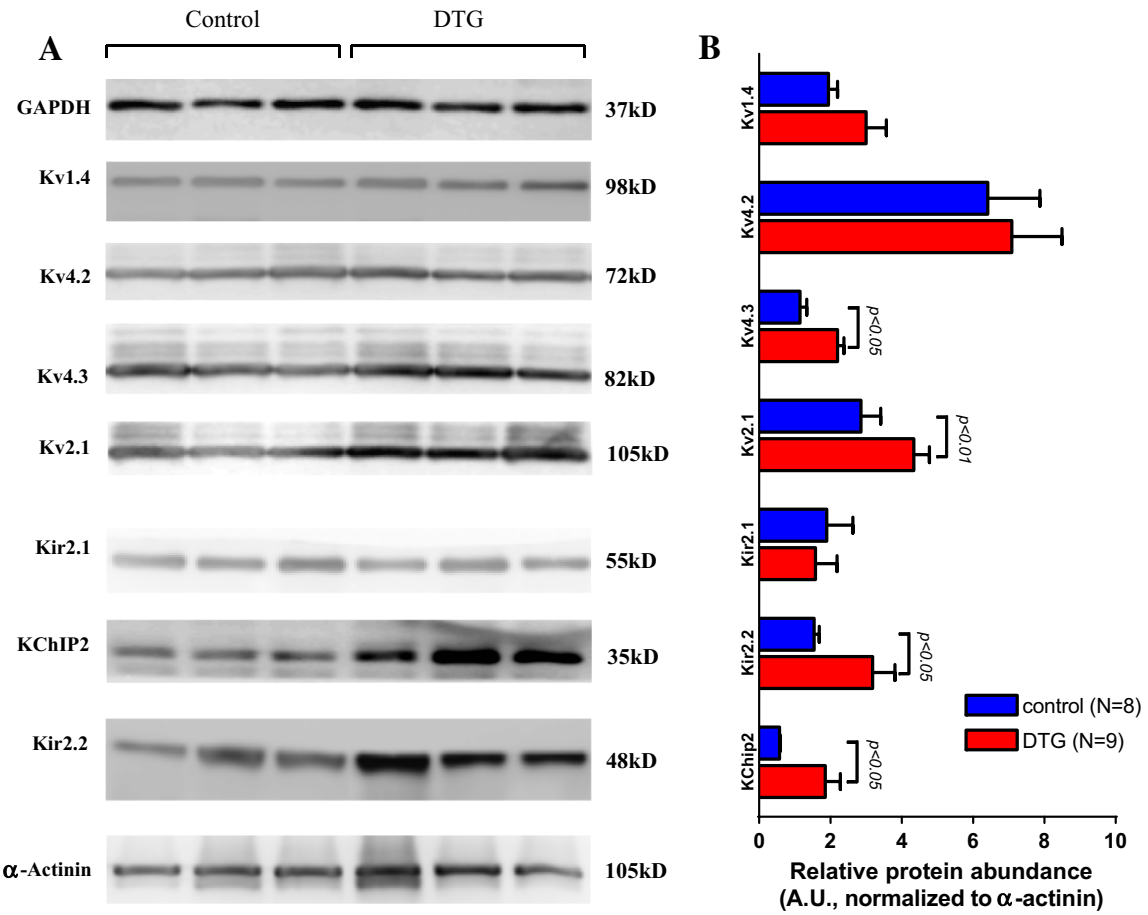

Fig. 5 The expression of potassium channels in control ($N = 8$) and DTG ($N = 9$) hearts. Representative Western blots of Kv1.4, Kv4.2, Kv4.3, Kv2.1, Kir2.1, KChiP2 and Kir2.2 (**a**) are shown. The averaged expression level was normalized to sarcomeric α-actinin (**b**)

myocytes. These results show that EADs and DADs can occur even in DTG myocytes with shortened APs.

Cavβ2a DTG mice had conduction abnormalities and arrhythmias

To determine if EADs and DADs in DTG myocytes were associated with arrhythmias, we further analyzed telemetric ECG recordings in control and DTG mice. Telemetric ECGs recorded in ambulatory mice showed no difference in heart rates between control and DTG mice but some episodes of arrhythmias. AV blocks and non-sustained ventricular tachycardia (VT) were found in 5 of 15 DTG mice but in none of control mice ($n = 12$) (Fig. 9b–g). Premature ventricular beats (PVC) were found in all 15 DTG mice but only occasionally in one of the 12 control mice (Fig. 9b, f). Non-sustained ventricular tachycardia (VT) was also observed in 0.27 ± 0.08 % of the total recorded time in those 5 DTG animals but not in any examined control mice (Fig. 9g). During the recording, one DTG mouse died of bradycardia (Supplemental Fig. 5).

Fibrosis of atrioventricular node (AVN) and myocardium in Cavβ2a DTG mice

We previously reported that there is severe fibrosis of the ventricular walls of Cavβ2a DTG hearts due to myocyte necrosis [25]. AV node fibrosis has been linked to AV blocks [11, 25]. Here we examined if AV node were fibrotic causing AV blocks (Fig. 10). In normal control mice, the AV node was surrounded with fibrous tissue that separates the AVN from the ventricles and no fibrosis was seen within the AV node (Fig. 10a). In contrast, the AV node of DTG hearts was fibrotic, which could contribute to AV block seen in DTG mice. In addition, Masson's trichrome staining showed little fibrosis in the atrial walls and ventricular walls of control mice but significant fibrosis in heart walls of the DTG mice (Fig. 10).

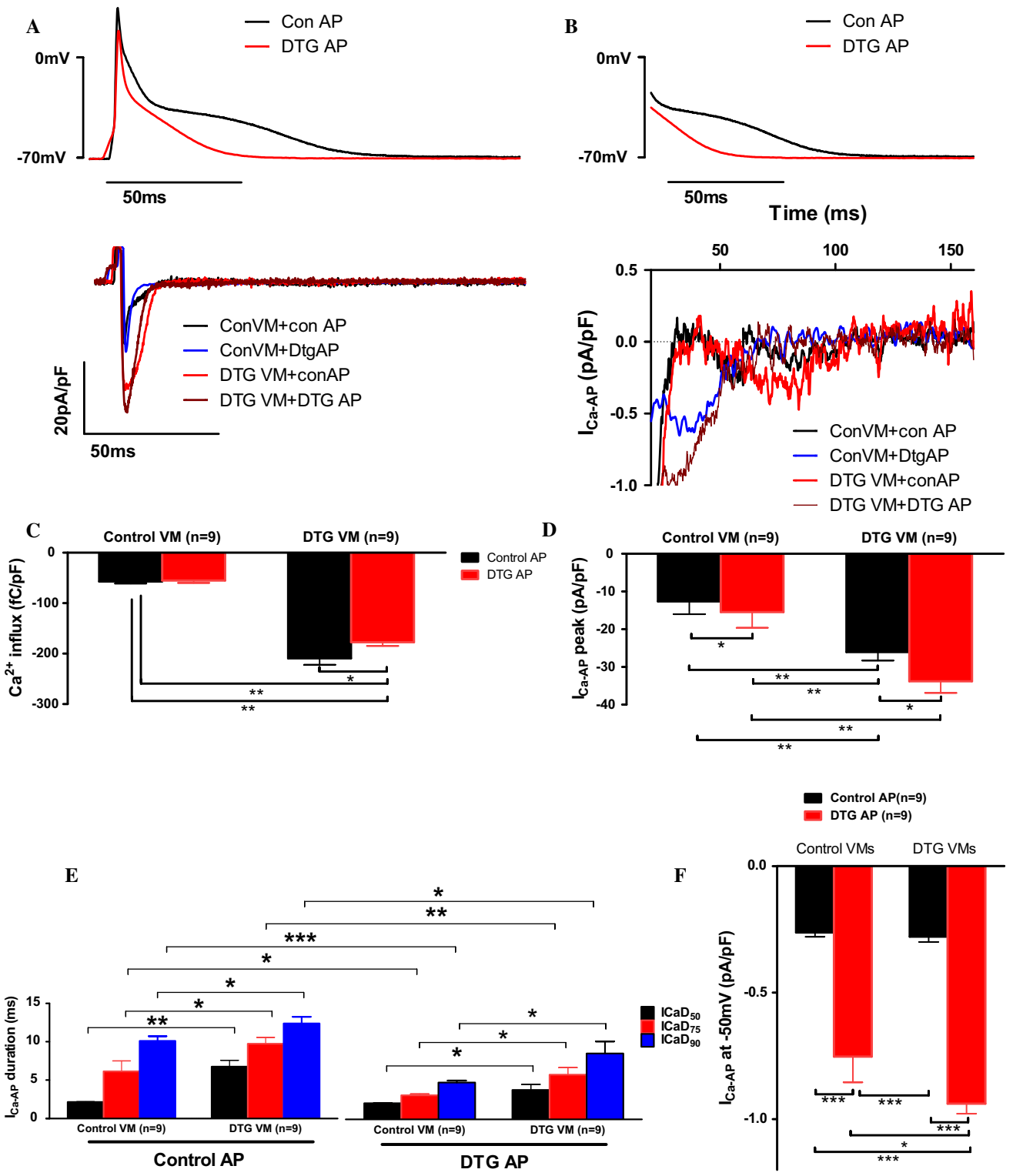

Fig. 6 Ca^{2+} currents under AP clamp ($I_{Ca\text{-}AP}$) with a typical control AP and a typical DTG AP. **a** Examples of raw $I_{Ca\text{-}AP}$ recorded in sodium-free and potassium-free solutions with AP clamp in a control and a DTG VM. **b** Expanded view of tail Ca^{2+} currents during the repolarizing phase of AP clamp. **c** Total Ca^{2+} influx through the Cav1.2 channel under AP clamp in control ($n = 9$, $N = 3$) and DTG ($n = 9$, $N = 3$) VMs. **d** The peak of $I_{Ca\text{-}AP}$ in control and DTG VMs. **e** $I_{Ca\text{-}AP}$ durations examined at 50, 75, and 90 % decay of $I_{Ca\text{-}AP}$. **f** The peak of the tail $I_{Ca\text{-}AP}$, usually at about −50 mV, the midpoint of AP phase 2 repolarization. There were significant greater tail currents when a shorter AP command was used on both control and DTG VMs. $^{*}p < 0.05$; $^{**}p < 0.01$; $^{***}p < 0.001$; two-way ANOVA with repeated measurements and post hoc *t* test was used

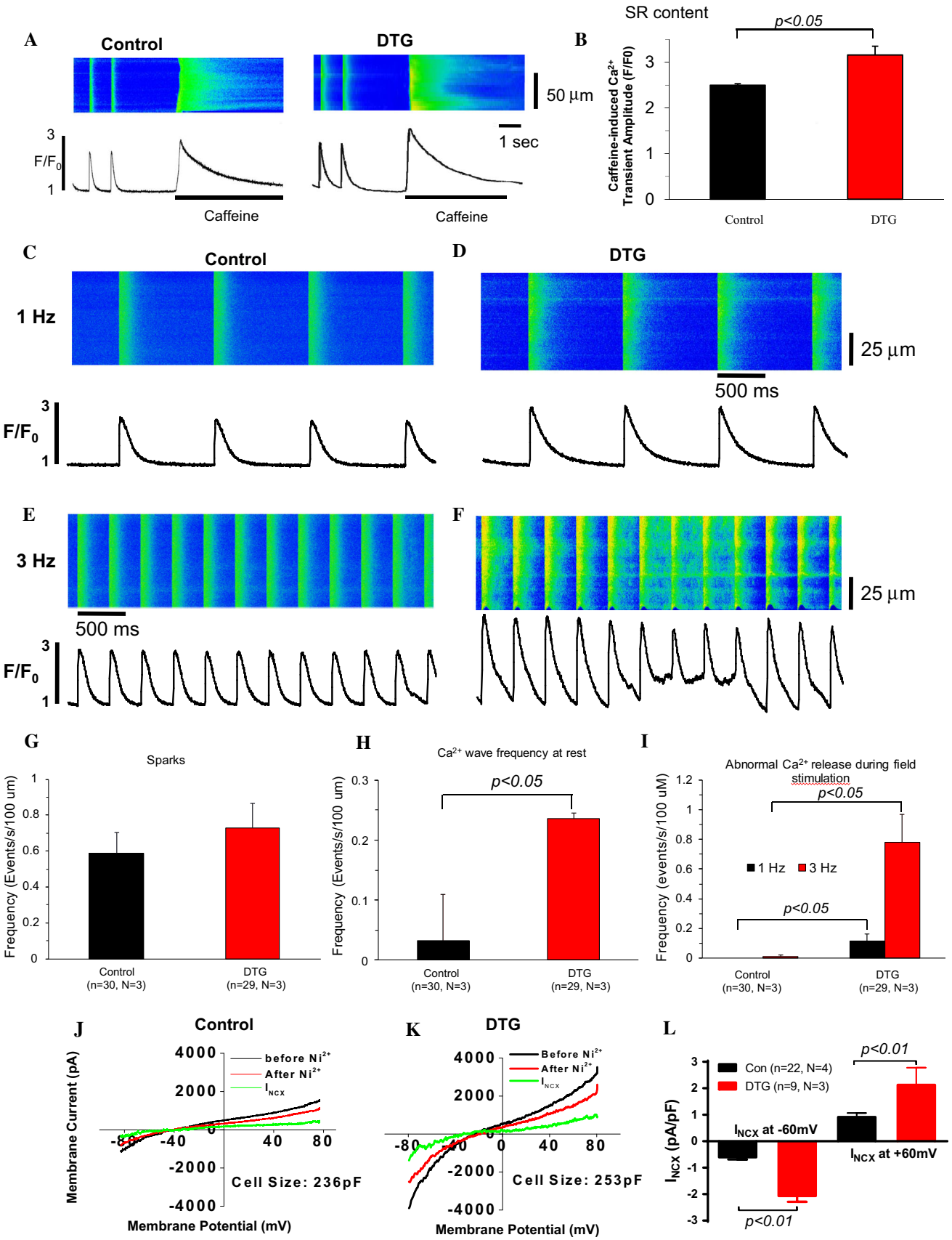
A
Control
DTG
50 µm
1 sec
3
F/F0
1
Caffeine
Caffeine
B
SR content
p<0.05
Caffeine-induced Ca2+ Transient Amplitude (F/F0)
3
2
1
0
Control
DTG
C
Control
1 Hz
3
F/F0
1
D
DTG
25 µm
500 ms
E
3 Hz
500 ms
3
F/F0
1
F
25 µm
G
Sparks
Frequency (Events/s/100 um)
1
0.8
0.6
0.4
0.2
0
Control
(n=30, N=3)
DTG
(n=29, N=3)
H
Ca2+ wave frequency at rest
p<0.05
Frequency (Events/s/100 um)
0.3
0.2
0.1
0
Control
(n=30, N=3)
DTG
(n=29, N=3)
I
Abnormal Ca2+ release during field stimulation
p<0.05
1 Hz
3 Hz
p<0.05
Frequency (events/s/100 uM)
1.2
1
0.8
0.6
0.4
0.2
0
Control
(n=30, N=3)
DTG
(n=29, N=3)
J
Control
Membrane Current (pA)
4000
2000
-2000
-4000
before Ni2+
After Ni2+
INCX
-80
-40
40
80
Cell Size: 236pF
Membrane Potential (mV)
K
DTG
4000
2000
-2000
-4000
Before Ni2+
After Ni2+
INCX
-80
0
40
80
Cell Size: 253pF
Membrane Potential (mV)
L
p<0.01
Con (n=22, N=4)
DTG (n=9, N=3)
INCX (pA/pF)
3
2
1
0
-1
-2
-3
INCX at -60mV
INCX at +60mV
p<0.01

◀**Fig. 7** β2a DTG VMs have diastolic Ca^{2+} leaks and Ca^{2+} waves due to SR Ca^{2+} overload and increased NCX activity. **a** Examples of caffeine induced Ca^{2+} transients following field stimulation induced Ca^{2+} transients in a control VM and a DTG VM. **b** The amplitudes of caffeine-induced Ca^{2+} transients, an index of SR Ca^{2+} content. **c**, **d** Examples of line-scanning Ca^{2+} transients induced by 1 Hz field-stimulation in control and DTG VMs. **e**, **f** Examples of line-scanning Ca^{2+} transients induced by 3 Hz field-stimulation in control and DTG VMs. **g** Ca^{2+} spark frequency at rest in control and DTG VMs. **h** Ca^{2+} wave frequencies at rest in DTG and control VMs. **i** Abnormal Ca^{2+} release, i.e., abnormal diastolic Ca^{2+} and decay as shown in control and DTG myocytes, during field stimulation. **j**, **k** Examples of raw currents recorded during a ramp test (+80 mV to −80 mV at 100 mV/s) before (*black line*) and after (*red line*) the application of 5 mM $NiCl_2$. The Ni^{2+}-sensitive currents (*green line*) were considered as I_{NCX}. **l** Averaged I_{NCX} at −60 and +60 mV showing increased I_{NCX} in DTG myocytes. $*p < 0.05$; $**p < 0.01$; $***p < 0.001$; unpaired *t* test (**b**, **g**, **h** and **l**) or two-way ANOVA with repeated measurements and post hoc *t* test (**i**) was used

Discussion

There is an interplay between the alterations of Ca^{2+} handling and electrical remodeling during the progression of heart disease. It is well known that the action potential profile, especially the phase 1 repolarization shaped by I_{to}, profoundly changes $I_{Ca\text{-}L}$, I_{NCX} and thus excitation–contraction coupling and intracellular Ca^{2+} transients [31]. Conversely, chronic increases of intracellular Ca^{2+} may decrease or increase the expression of transient outward potassium currents (I_{to}) depending on the animal system studied and the time when the animal is studied [28, 30]. Decreases in intracellular Ca^{2+} enhances the expression of the L-type Ca^{2+} channel [32]. Increases in Cav1.2 activity may lead to prolongation of the action potential duration

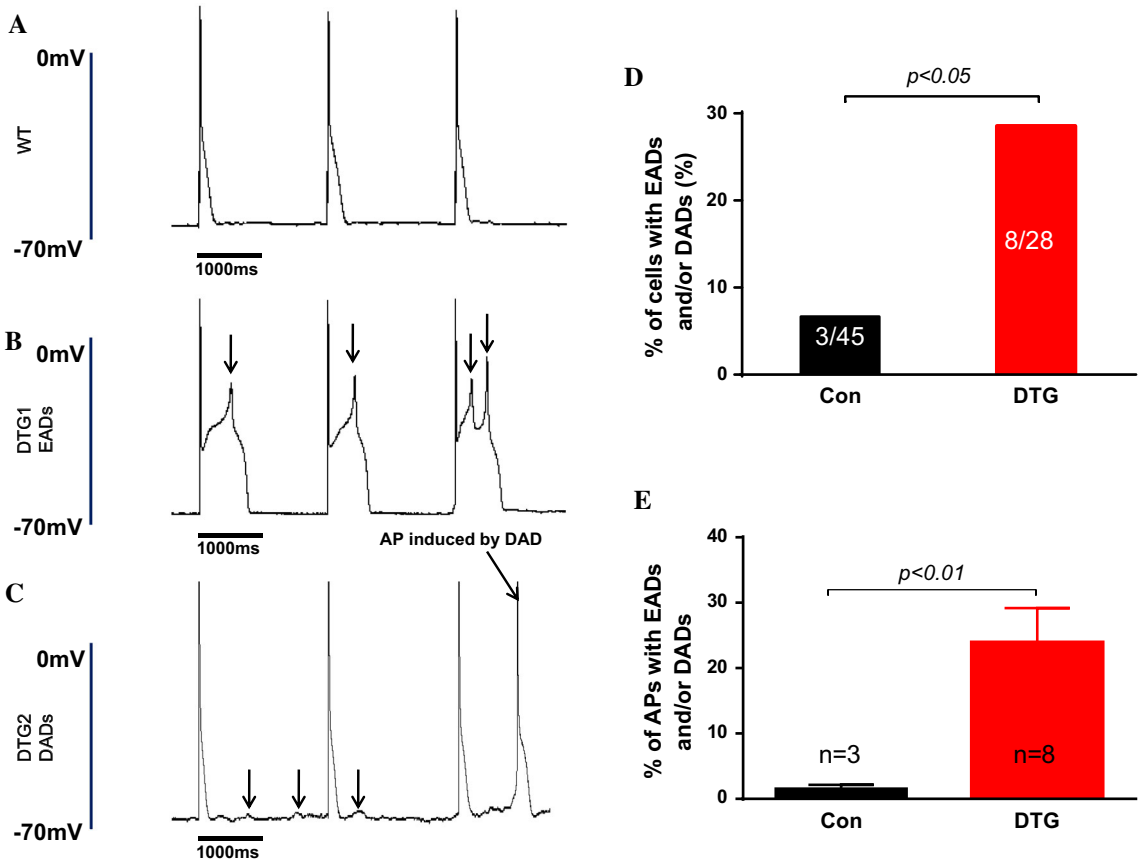

Fig. 8 A greater proportion of DTG myocytes have early and/or delayed afterdepolarizations (EADs and/or DADs). Action potentials recorded from one control (**a**) and two DTG (**b**, **c**) VMs, showing EADs and DADs (*arrows*) in DTG myocytes. **d** A greater proportion of DTG myocytes have EADs and/or DADs than control myocytes. *p* value was determined by contingency table analysis. **e** The percentage of APs having EADs or DADs in the 3 control VMs with EADs and/or DADs and 8 DTG VMs. VMs were from 5 control and 5 DTG animals

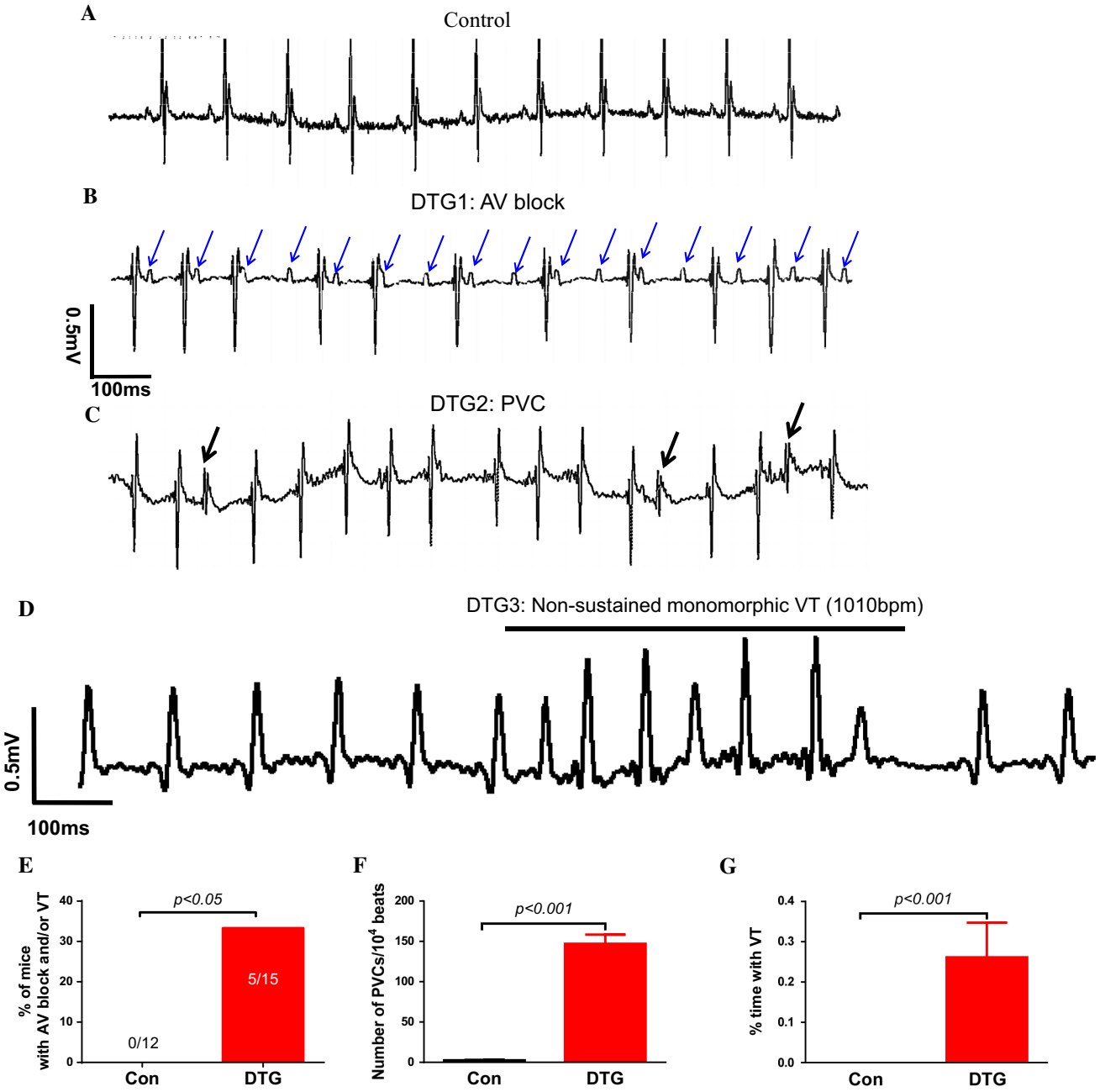

Fig. 9 DTG mice have ventricular arrhythmias. **a** Telemetric ECG from a control mouse. **b** Complete AV block in a DTG mouse. The *arrows* indicate *p* waves. **c** Extrasystole/PVC (*arrows*) recorded from a DTG mouse. **d** Non-sustained VT in a DTG mice. **e** The incidence rate of mice with AV block and/or VT in control ($N = 12$) and DTG ($N = 15$) mice. **f** The numbers of PVCs in every 10^4 heart beats in control mice ($N = 12$) and DTG mice with PVCs ($N = 5$). **g** The percentage of time with VT in control ($N = 12$) and DTG ($N = 5$) mice. Unpaired student *t* test was performed for **f** and **g**

and abnormal Ca^{2+} handling, both contributing to arrhythmogenicity [2, 3, 20]. In this study, we induced a marked and persistent increase in Cav1.2 influx [25] similar to that seen in diseased hearts due to prolongation of action potential [1, 6, 22], chronic activation of the β-adrenergic system [9] and molecular remodeling [12, 21], which may result in cellular Ca^{2+} overload. We found that these mice had shorter than normal QT intervals and AP durations despite of increased Cav1.2 activity. The shortened QT intervals and APD were caused by significant increases in potassium currents and channel expression. The alteration of action potential duration profoundly affects the time course and Ca^{2+} influx mediated by $I_{Ca\text{-}L}$ [1, 6, 22]. However, shortened APD and increasing NCX activity did not effectively limit Ca^{2+} influx and Cavβ2a overexpression still causes SR Ca^{2+} overload and

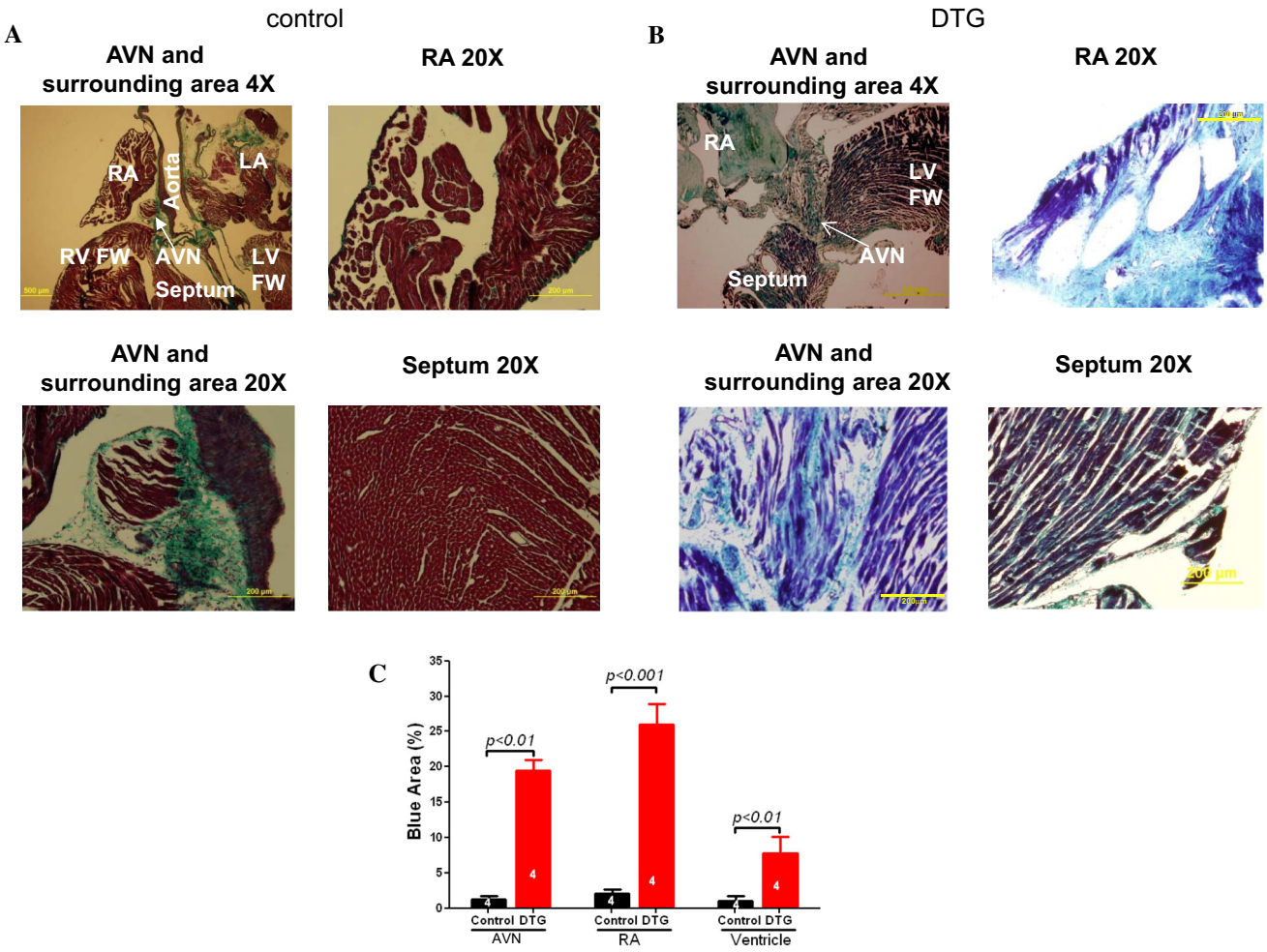

Fig. 10 DTG mice have extensive fibrosis in the atria, AV node (AVN) and ventricles. **a** and **b** Masson's trichrome staining of the heart sections of a control mouse (**a**) and a DTG mouse (**b**). The blue staining is fibrosis. **c** Quantitation of fibrotic area in the AV node, right atrium (RA) and ventricles. Two-way ANOVA with post hoc *t* test (Bonferroni adjustment) was performed for Fig. 10c. Four control and 4 DTG hearts were studied. *RA* right atrium, *LA* left atrium, *RV* right ventricle, *LV* left ventricle, *FW* free wall, *AVN* atrioventricular node

spontaneous Ca^{2+} release, EADs and DADs, and arrhythmias in Cavβ2a DTG mice. SR Ca^{2+} overload also results in fibrosis of AV node and myocardium to cause conduction abnormalities. These results show that cardiac myocytes are capable of sensing persistent increases in Ca^{2+} influx through Cav1.2 and remodeling to reduce Ca^{2+} influx but it may not be adequate in Cavβ2a DTG myocytes.

Does enhanced Cav1.2 activity always prolong QT and myocyte action potentials?

The Cav1.2 channel plays a critical role in triggering Ca^{2+} release from the SR in cardiac myocytes, and mediates a depolarizing current during the plateau phase (phase 2) of the action potential [7]. The balance between depolarizing currents (mainly I_{Ca}) and repolarizing K^+ currents determines the duration of the plateaus phase of the AP in large mammals [26]. A prolongation of the AP occurs when Cav1.2 properties change to increase Ca^{2+} current (e.g., the mutation in Timothy syndrome [4]), and repolarizing potassium currents are not changed. In the Cavβ2a transgenic mice, a reactive increase in repolarizing potassium currents overwhelmed the increases in Cav1.2 activity to shorten the AP durations and QT intervals. Previously, it has been shown that in 4- to 8-month-old transgenic mice overexpressing a Cav1.2α_{1C}, I_{to} and I_{Ksus} in myocytes were increased but APD was not shortened [8]. This discrepancy could be because there is greater increase in $I_{Ca\text{-}L}$ and probably more electrical remodeling in our animal model. In good agreement, in Cav1.2α1c heterozygous knockout myocytes with reduced $I_{Ca\text{-}L}$, the action potential duration was prolonged (Supplemental Fig. 6 A, B) when compared to wild type control myocytes. The maximal phase 1

repolarization rate, total I_K, 4-AP-insensitive and 4-AP-sensitive I_K were decreased in the heterozygous knockout myocyte (Supplemental Fig. 6C-F). In a transgenic mouse model overexpressing CaMK II peptide inhibitor (Ac3-I) [23], both Cav1.2 activity and I_{to} expression are increased.

The condition of the heart and the extent of increases in Ca^{2+} influx also affect the action potential duration. In the mice overexpressing Cav1.2α1c, I_{to} was increased at the age of 4 months when the heart was in early stage of hypertrophy but decreased at the age of 9–12 months when the heart was in advanced hypertrophic stage [8]. We studied K^+ currents in mice overexpressing Cav1.2β2a at high level at the age of 6 months when depressed cardiac function was present [11, 25]. In these myocytes, 4-AP-insensitive K^+ currents returned to normal but I_{to} was reduced compared to those in age-matched control and LE DTG myocytes (Supplemental Fig. 7).

At last, the way of increasing Ca^{2+} influx through Cav1.2 may also have effects on action potential duration. The mutation of G406R in Timothy syndrome does not significantly increase the amplitude of $I_{Ca\text{-}L}$ but it dramatically slows down the inactivation of $I_{Ca\text{-}L}$, which causes significant prolongation of the APD [15] and arrhythmias [16]. This is different from our transgenic mouse model in which the $I_{Ca\text{-}L}$ amplitude is significantly increased but $I_{Ca\text{-}L}$ inactivation is not significantly different compared to control $I_{Ca\text{-}L}$. Whether this difference could result in a different phenotype of our mouse model than the Timothy syndrome model needs to be further studied.

How does increased Ca^{2+} influx induce increased potassium currents?

Our study shows that persistent increases in Ca^{2+} influx through the Cav1.2 channel leads to electrical remodeling with an increase in potassium channel abundance and a subsequent decrease in the APD and QT interval. It has been reported that the activation of the calcineurin/NFAT signaling cascade by increased cytosolic Ca^{2+} is able to upregulate the expression of Kv4.2 channels but not Kv1.4, Kv4.3 and KChIP2 [18]. Calcineurin is activated in the Cavβ2a transgenic mouse [11] and thus this could mediate the upregulation of Kv4.2 we observed. In contrast, it has been reported that increases in Ca^{2+} influx through Cav1.2 in cultured myocytes decreases I_{to} expression in a calcineurin-dependent manner [28], and higher calcineurin activity in the endomyocardium may promote lower Kv4.2 channel expression in endomyocardium [30]. In our transgenic mice, the expression of multiple potassium channels (Kv1.4, Kv4.3, Kv2.1, Kir2.2, and KChIP2) is upregulated, thus it is possible that different mechanisms are involved. What seems clear is that there is a mechanism that "senses" persistently increased Ca^{2+} influx through the LTCC and results in an adaptive shortening in APD via increasing the expression of K^+ channels, intending to limit excessive Ca^{2+} entry.

Another possibility is that increased Ca^{2+} influx [11] activates CaMK II, which then enhances potassium channel activity [27]. Acute overexpression of CaMK IIδ may increase I_{K1} density [27], but chronic CaMK II inhibition by an overxpressed peptide (Ac-3I) in a mouse model increases I_{to} and I_{K1} expression [23]. Li et al. [23] and others [36] show that decreased SR Ca^{2+} content could be the central point for the upregulation of potassium channel expression. In our study, the SR content is increased along with potassium channel expression, indicating a complex modulation of potassium channel expression by SR content.

Can AP shortening effectively reduce arrhythmogenic activities in Cavβ2a DTG myocytes and mice?

Prolongation of the QT interval and myocyte action potential is clearly linked to lethal ventricular arrhythmias in humans [20]. Alterations in RyR properties without changing action potential profiles [24] and abnormal SR Ca^{2+} release are also linked to sudden cardiac death [29]. Our results show that increasing Ca^{2+} influx through the LTCC causes electrophysiological remodeling that shortens the APD. However, the shortening of the APD does not effectively limit Ca^{2+} influx into the myocytes and SR Ca^{2+} overload still occurs. Furthermore, AP shortening may decrease the refractory period and promote arrhythmias, especially when abnormal Ca^{2+} release in DTG myocytes causes EADs and DADs. In addition, SR Ca^{2+} overload may induce myocyte death, myocardial fibrosis [11, 14, 25], and AV node fibrosis, providing the substrates for arrhythmias and conduction blocks. Thus the affected mice showed multiple types of cardiac arrhythmias, AV blocks and die prematurely of sudden death. Collectively our results suggest that SR Ca^{2+} overload can induce lethal arrhythmias without requiring AP prolongation.

Conclusion

Taking all these results together, our study support the notion that when Ca^{2+} current is modified, K^+ currents change to ensure an appropriate balance between depolarizing and repolarizing currents, which leads to alterations of action potential profile and adjustment to excitation contraction coupling. However, in the face of significant increase of Ca^{2+} influx, the increases of K^+ currents and resultant shortening of action potentials are protective but

may not be adequate for preventing SR Ca^{2+} overload, abnormal SR Ca^{2+} release, myocyte death and fibrosis, conduction blocks and arrhythmias. It seems that normalization of Ca^{2+} handling is critical for arrhythmia prevention.

Limitations

Although our data support that arrhythmias are the most likely cause of death of the Cavβ2a DTG mice, we could not rule out the possibility that alterations of cardiac structure of the atria and ventricles cause stroke to kill DTG mice. Additionally, action potential duration varies within different layers of myocardium. In our study, we did not characterize action potentials in myocytes from different layers of myocardium and could not tell the extent of the shortening of APs in different myocardial layers. Nonetheless, shortened QT indicates that ventricular myocyte action potentials were shortened on average. At last, there are fundamental differences in cardiac electrophysiology and myocyte Ca^{2+} handling between humans and mice [27]. Thus, extrapolating our results from our mouse model to humans should be done cautiously.

Compliance with ethical standards

Conflict of interest None.

Funding sources This study was supported by NIH and HMMI grants to JDM, NIH HL088243 and AHA 0730347N to XC.

References

1. Aiba T, Tomaselli GF (2010) Electrical remodeling in the failing heart. Curr Opin Cardiol 25:29–36. doi:10.1097/HCO.0b013e328333d3d6
2. Anderson ME (2004) Calmodulin kinase and L-type calcium channels; a recipe for arrhythmias? Trends Cardiovasc Med 14:152–161. doi:10.1016/j.tcm.2004.02.005
3. Antoons G, Sipido KR (2008) Targeting calcium handling in arrhythmias. Europace 10:1364–1369. doi:10.1093/europace/eun271
4. Barrett CF, Tsien RW (2008) The Timothy syndrome mutation differentially affects voltage- and calcium-dependent inactivation of CaV1.2 L-type calcium channels. Proc Natl Acad Sci USA 105:2157–2162. doi:10.1073/pnas.0710501105
5. Barry DM, Nerbonne JM (1996) Myocardial potassium channels: electrophysiological and molecular diversity. Annu Rev Physiol 58:363–394. doi:10.1146/annurev.ph.58.030196.002051
6. Bassani RA, Altamirano J, Puglisi JL, Bers DM (2004) Action potential duration determines sarcoplasmic reticulum Ca2+ reloading in mammalian ventricular myocytes. J Physiol 559:593–609. doi:10.1113/jphysiol.2004.067959
7. Bers DM (2002) Cardiac excitation–contraction coupling. Nature 415:198–205. doi:10.1038/415198a
8. Bodi I, Muth JN, Hahn HS, Petrashevskaya NN, Rubio M, Koch SE, Varadi G, Schwartz A (2003) Electrical remodeling in hearts from a calcium-dependent mouse model of hypertrophy and failure: complex nature of K+ current changes and action potential duration. J Am Coll Cardiol 41:1611–1622. doi:10.1016/S0735-1097(03)00244-4
9. Bristow MR, Kantrowitz NE, Ginsburg R, Fowler MB (1985) Beta-adrenergic function in heart muscle disease and heart failure. J Mol Cell Cardiol 17(Suppl 2):41–52. doi:10.1016/0022-2828(85)90007-0
10. Chen J, Piper DR, Sanguinetti MC (2002) Voltage sensing and activation gating of HCN pacemaker channels. Trends Cardiovasc Med 12:42–45 doi: S1050173801001414 [pii]
11. Chen X, Nakayama H, Zhang X, Ai X, Harris DM, Tang M, Zhang H, Szeto C, Stockbower K, Berretta RM, Eckhart AD, Koch WJ, Molkentin JD, Houser SR (2011) Calcium influx through Cav1.2 is a proximal signal for pathological cardiomyocyte hypertrophy. J Mol Cell Cardiol 50:460–470. doi:10.1016/j.yjmcc.2010.11.012
12. Chen X, Piacentino V 3rd, Furukawa S, Goldman B, Margulies KB, Houser SR (2002) L-type Ca2+ channel density and regulation are altered in failing human ventricular myocytes and recover after support with mechanical assist devices. Circ Res 91:517–524. doi:10.1161/01.RES.0000033988.13062.7C
13. Chen X, Wilson RM, Kubo H, Berretta RM, Harris DM, Zhang X, Jaleel N, MacDonnell SM, Bearzi C, Tillmanns J, Trofimova I, Hosoda T, Mosna F, Cribbs L, Leri A, Kajstura J, Anversa P, Houser SR (2007) Adolescent feline heart contains a population of small, proliferative ventricular myocytes with immature physiological properties. Circ Res 100:536–544. doi:10.1161/01.RES.0000259560.39234.99
14. Chen X, Zhang X, Kubo H, Harris DM, Mills GD, Moyer J, Berretta R, Potts ST, Marsh JD, Houser SR (2005) Ca2+ influx-induced sarcoplasmic reticulum Ca2+ overload causes mitochondrial-dependent apoptosis in ventricular myocytes. Circ Res 97:1009–1017. doi:10.1161/01.RES.0000189270.72915.D1
15. Cheng EP, Yuan C, Navedo MF, Dixon RE, Nieves-Cintron M, Scott JD, Santana LF (2011) Restoration of normal L-type Ca2+ channel function during Timothy syndrome by ablation of an anchoring protein. Circ Res 109:255–261. doi:10.1161/CIRCRESAHA.111.248252
16. Drum BM, Dixon RE, Yuan C, Cheng EP, Santana LF (2014) Cellular mechanisms of ventricular arrhythmias in a mouse model of Timothy syndrome (long QT syndrome 8). J Mol Cell Cardiol 66:63–71. doi:10.1016/j.yjmcc.2013.10.021
17. Fozzard HA (1992) Afterdepolarizations and triggered activity. Basic Res Cardiol 87(Suppl 2):105–113
18. Gong N, Bodi I, Zobel C, Schwartz A, Molkentin JD, Backx PH (2006) Calcineurin increases cardiac transient outward K+ currents via transcriptional up-regulation of Kv4.2 channel subunits. J Biol Chem 281:38498–38506. doi:10.1074/jbc.M607774200
19. Goonasekera SA, Hammer K, Auger-Messier M, Bodi I, Chen X, Zhang H, Reiken S, Elrod JW, Correll RN, York AJ, Sargent MA, Hofmann F, Moosmang S, Marks AR, Houser SR, Bers DM, Molkentin JD (2012) Decreased cardiac L-type Ca(2)(+) channel activity induces hypertrophy and heart failure in mice. J Clin Invest 122:280–290. doi:10.1172/JCI58227
20. Hedley PL, Jorgensen P, Schlamowitz S, Wangari R, Moolman-Smook J, Brink PA, Kanters JK, Corfield VA, Christiansen M (2009) The genetic basis of long QT and short QT syndromes: a mutation update. Hum Mutat 30:1486–1511. doi:10.1002/humu.21106
21. Hullin R, Khan IF, Wirtz S, Mohacsi P, Varadi G, Schwartz A, Herzig S (2003) Cardiac L-type calcium channel beta-subunits expressed in human heart have differential effects on single

channel characteristics. J Biol Chem 278:21623–21630. doi:10.1074/jbc.M211164200
22. Janczewski AM, Spurgeon HA, Lakatta EG (2002) Action potential prolongation in cardiac myocytes of old rats is an adaptation to sustain youthful intracellular Ca2+ regulation. J Mol Cell Cardiol 34:641–648. doi:10.1006/jmcc.2002.2004
23. Li J, Marionneau C, Zhang R, Shah V, Hell JW, Nerbonne JM, Anderson ME (2006) Calmodulin kinase II inhibition shortens action potential duration by upregulation of K+ currents. Circ Res 99:1092–1099. doi:10.1161/01.RES.0000249369.71709.5c
24. Liu N, Colombi B, Memmi M, Zissimopoulos S, Rizzi N, Negri S, Imbriani M, Napolitano C, Lai FA, Priori SG (2006) Arrhythmogenesis in catecholaminergic polymorphic ventricular tachycardia: insights from a RyR2 R4496C knock-in mouse model. Circ Res 99:292–298. doi:10.1161/01.RES.0000235869.50747.e1
25. Nakayama H, Chen X, Baines CP, Klevitsky R, Zhang X, Zhang H, Jaleel N, Chua BH, Hewett TE, Robbins J, Houser SR, Molkentin JD (2007) Ca2+- and mitochondrial-dependent cardiomyocyte necrosis as a primary mediator of heart failure. J Clin Invest 117:2431–2444. doi:10.1172/JCI31060
26. Nerbonne JM (2000) Molecular basis of functional voltage-gated K+ channel diversity in the mammalian myocardium. J Physiol 525 Pt 2:285–298. doi: PHY_0696 [pii]
27. Nerbonne JM (2004) Studying cardiac arrhythmias in the mouse—a reasonable model for probing mechanisms? Trends Cardiovasc Med 14:83–93. doi:10.1016/j.tcm.2003.12.006
28. Perrier E, Perrier R, Richard S, Benitah JP (2004) Ca2+ controls functional expression of the cardiac K+ transient outward current via the calcineurin pathway. J Biol Chem 279:40634–40639. doi:10.1074/jbc.M407470200
29. Pogwizd SM, Schlotthauer K, Li L, Yuan W, Bers DM (2001) Arrhythmogenesis and contractile dysfunction in heart failure: roles of sodium–calcium exchange, inward rectifier potassium current, and residual beta-adrenergic responsiveness. Circ Res 88:1159–1167. doi:10.1161/hh1101.091193
30. Rossow CF, Dilly KW, Santana LF (2006) Differential calcineurin/NFATc3 activity contributes to the Ito transmural gradient in the mouse heart. Circ Res 98:1306–1313. doi:10.1161/01.RES.0000222028.92993.10
31. Sah R, Ramirez RJ, Oudit GY, Gidrewicz D, Trivieri MG, Zobel C, Backx PH (2003) Regulation of cardiac excitation-contraction coupling by action potential repolarization: role of the transient outward potassium current (I(to)). J Physiol 546:5–18. doi:10.1113/jphysiol.2002.026468
32. Schroder E, Magyar J, Burgess D, Andres D, Satin J (2007) Chronic verapamil treatment remodels ICa, L in mouse ventricle. Am J Physiol Heart Circ Physiol 292:H1906–H1916. doi:10.1152/ajpheart.00793.2006
33. Song LS, Sham JS, Stern MD, Lakatta EG, Cheng H (1998) Direct measurement of SR release flux by tracking 'Ca2+ spikes' in rat cardiac myocytes. J Physiol 512(Pt 3):677–691. doi:10.1111/j.1469-7793.1998.677bd.x
34. Stroud DM, Gaussin V, Burch JB, Yu C, Mishina Y, Schneider MD, Fishman GI, Morley GE (2007) Abnormal conduction and morphology in the atrioventricular node of mice with atrioventricular canal targeted deletion of Alk3/Bmpr1a receptor. Circulation 116:2535–2543. doi:10.1161/CIRCULATIONAHA.107.696583
35. Tang M, Zhang X, Li Y, Guan Y, Ai X, Szeto C, Nakayama H, Zhang H, Ge S, Molkentin JD, Houser SR, Chen X (2010) Enhanced basal contractility but reduced excitation-contraction coupling efficiency and beta-adrenergic reserve of hearts with increased Cav1.2 activity. Am J Physiol Heart Circ Physiol 299:H519–H528. doi:10.1152/ajpheart.00265.2010
36. Xu Y, Zhang Z, Timofeyev V, Sharma D, Xu D, Tuteja D, Dong PH, Ahmmed GU, Ji Y, Shull GE, Periasamy M, Chiamvimonvat N (2005) The effects of intracellular Ca2+ on cardiac K+ channel expression and activity: novel insights from genetically altered mice. J Physiol 562:745–758. doi:10.1113/jphysiol.2004.076216